Supplemental Information

Impaired angiopoietin/Tie2 signaling compromises Schlemm's canal integrity and induces glaucoma

Jaeryung Kim, Dae-Young Park, Hosung Bae, Do Young Park, Dongkyu Kim, Choong-kun Lee, Sukhyun Song, Tae-Young Chung, Dong Hui Lim, Yoshiaki Kubota, Young-Kwon Hong, Yulong He, Hellmut G. Augustin, Guillermo Oliver, Gou Young Koh

It includes;

1. Supplemental Figures 1-9 and their legends
2. Supplemental Tables 1-2

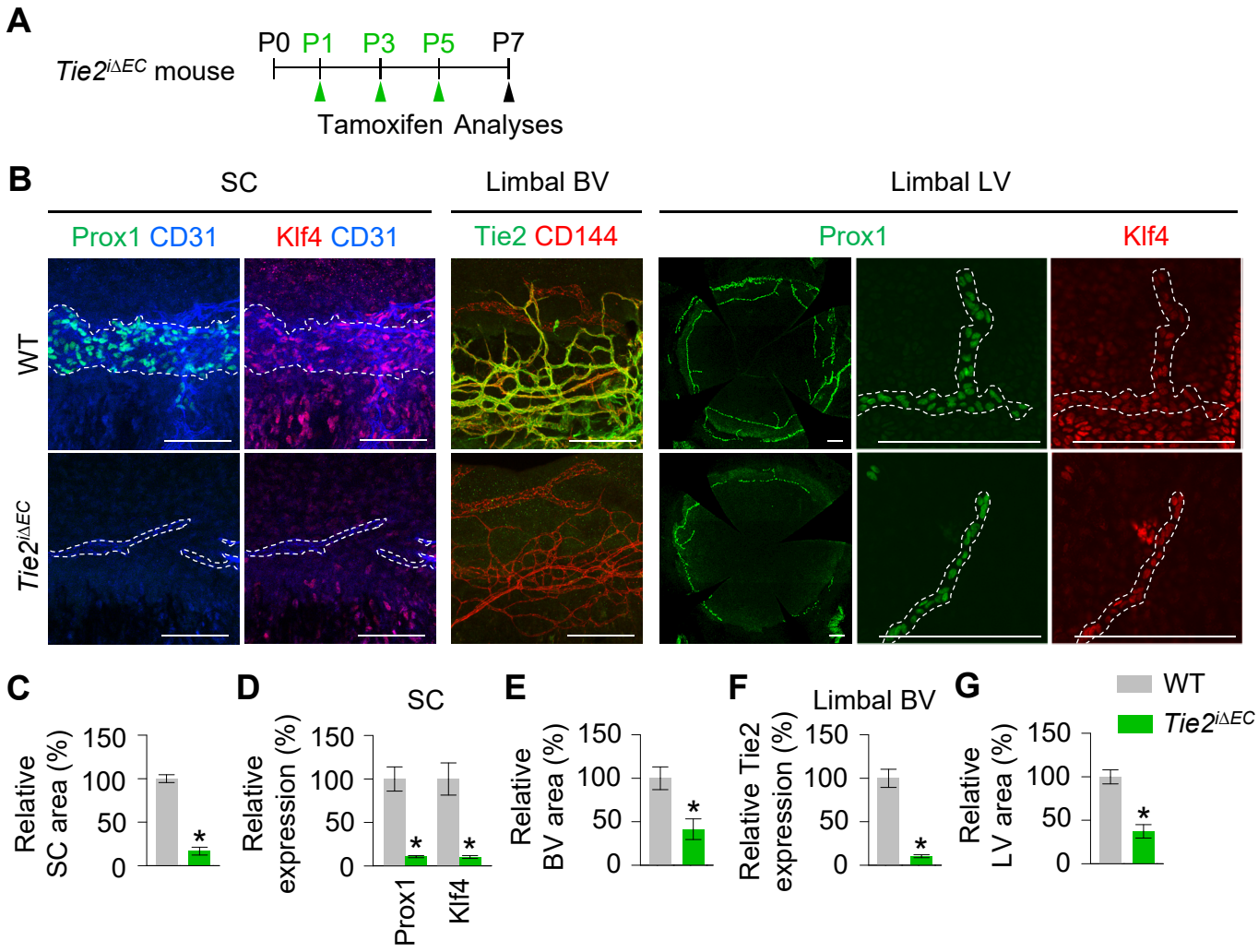

Supplemental Figure 1. Tie2 is indispensable for SC formation. (**A**) Diagram for EC-specific depletion of Tie2 in SC and corneal limbal vessels starting at P1 and analyses at P7 using *Tie2*$^{i\Delta EC}$ mice. (**B-G**) Images and comparisons of relative area and intensities of Prox1 and Klf4 immunostaining in CD31$^+$ SC, Tie2 immunostaining in CD144$^+$ limbal BVs, and Prox1 and Klf4 immunostaining in limbal LVs. Dashed lines demarcate the margins of SC or limbal LV. Limbal LV area was calculated as total Prox1$^+$ area at corneal limbus. Scale bars: 100 μm (SC and limbal BV); 200 μm (limbal LV). SC, limbal BV and LV area, and expression of each molecule in WT mice are normalized to 100%, and their relative levels in *Tie2*$^{i\Delta EC}$ mice are presented. Each group, $n = 4$. *$P < 0.05$ versus WT by Mann-Whitney *U* test.

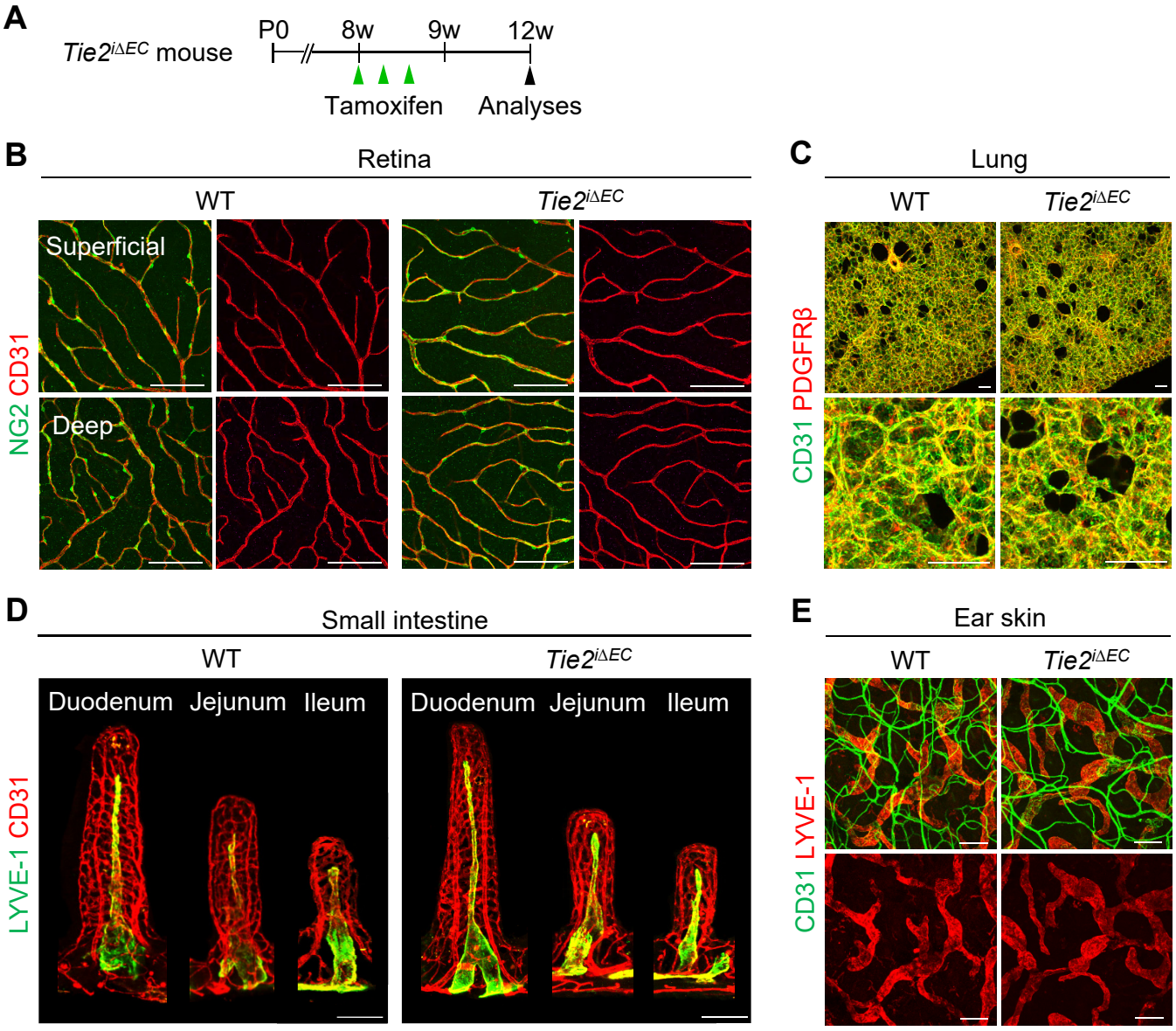

Supplemental Figure 2. No apparent change occurred in vessels of other organs by Tie2 depletion during adulthood. (**A**) Diagram for EC-specific depletion of Tie2 in SC starting at 8-week-old mice and analyses 4 weeks later using *Tie2*$^{i\Delta EC}$ mice. (**B**) Images showing CD31$^+$ BVs and NG2$^+$ pericytes in the superficial and deep vascular plexus of retina. (**C**) Images showing CD31$^+$ BVs and PDGFRβ$^+$ pericytes in lung. (**D**) Images showing CD31$^+$ BVs and LYVE-1$^+$ lacteals in small intestinal villi. (**E**) Images showing CD31$^+$ BVs and LYVE-1$^+$ LVs in ear skin. Scale bars: 100 μm.

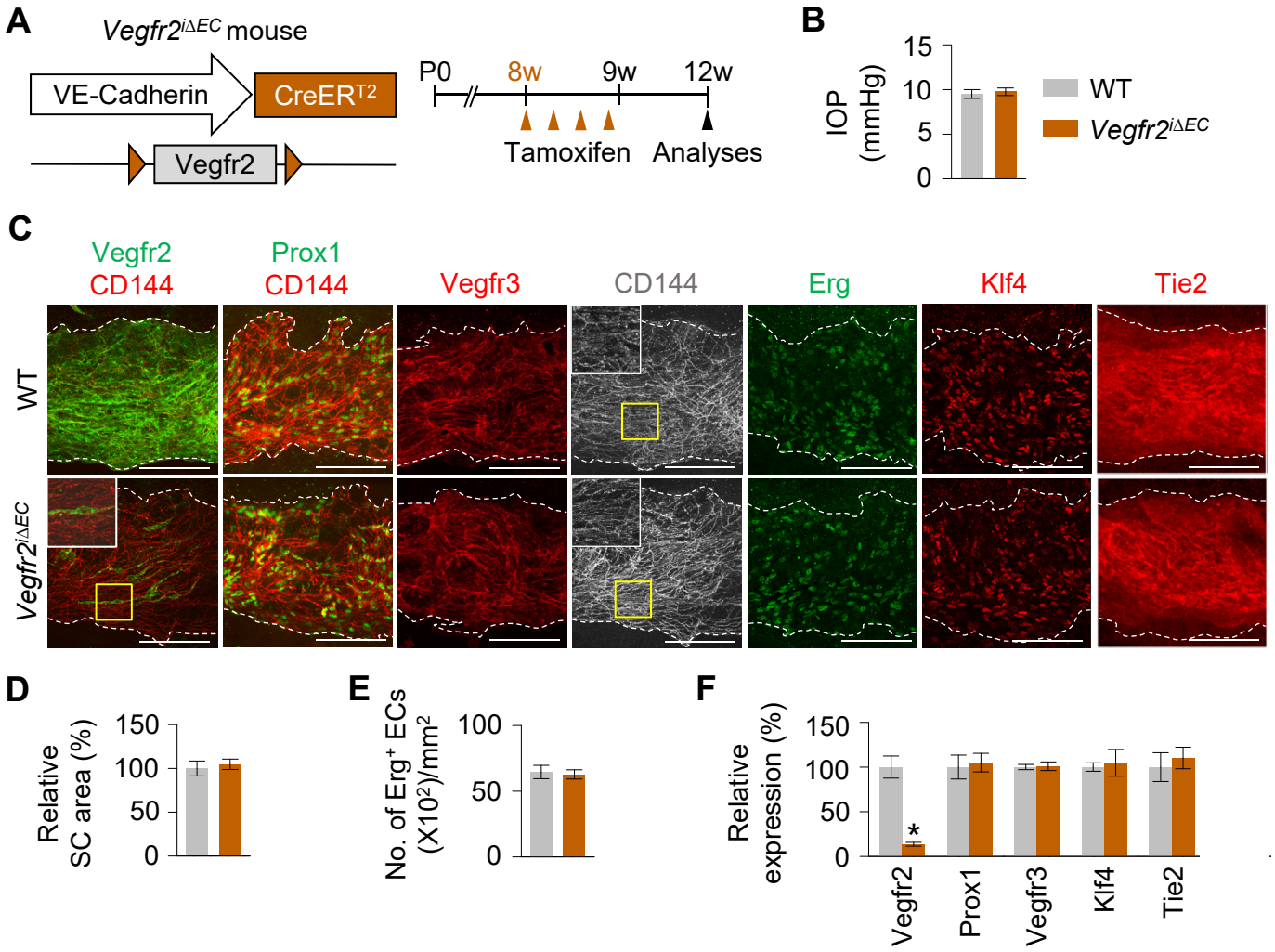

Supplemental Figure 3. Vegfr2 is not required for SC maintenance. (**A**) Diagram for EC-specific depletion of Vegfr2 in SC starting at 8-week-old mice and analyses 4 weeks later using *Vegfr2*$^{i\Delta EC}$ mice. (**B-F**) Images and comparisons of IOP, relative area, number of Erg$^+$ ECs, and intensities of Vegfr2, Prox1, Vegfr3, Klf4, and Tie2 immunostaining in CD144$^+$ SC. Dashed lines demarcate the margins of SC, and each area marked by a yellow box is magnified in the top left corner. Scale bars: 100 μm. SC area and expression of each molecule in WT mice are normalized to 100%, and their relative levels in *Vegfr2*$^{i\Delta EC}$ mice are presented. Each group, $n = 4$. *$P < 0.05$ versus WT by Mann-Whitney *U* test.

Supplemental Figure 4

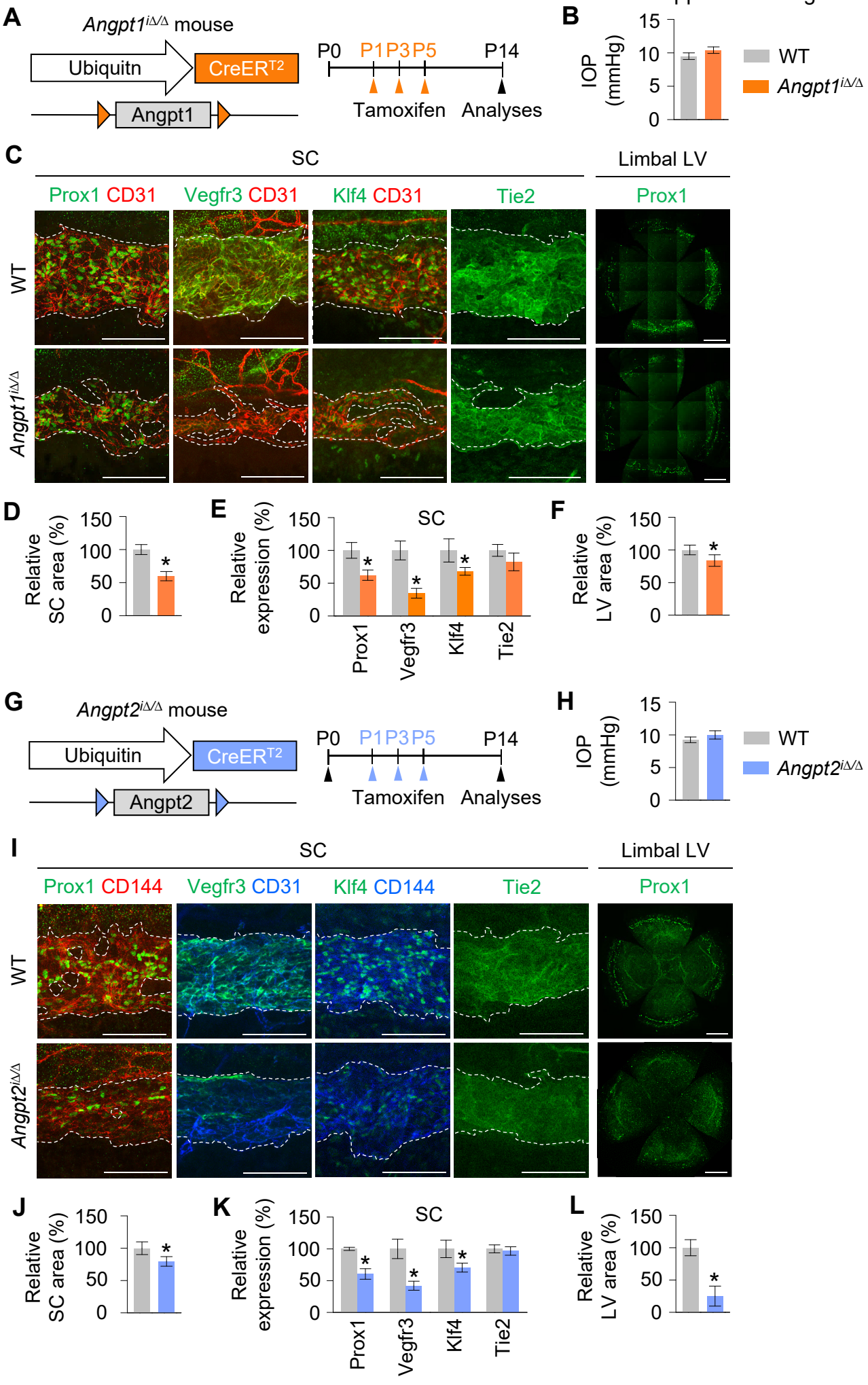

Supplemental Figure 4. Single depletion of Angpt1 or Angpt2 partially impairs SC formation during postnatal development. (**A** and **G**) Diagram for global depletion of Angpt1 or Angpt2 starting at P1 and analyses at P14 using *Angpt1*$^{i\Delta/\Delta}$ or *Angpt2*$^{i\Delta/\Delta}$ mice. (**B**-**F** and **H**-**L**) Images and comparisons of IOP, relative area, and intensities of Prox1, VEGFR3, Klf4, and Tie2 immunostaining in CD31$^+$ or CD144$^+$ SC and limbal LV. Dashed lines demarcate the margins of SC. Limbal LV area was calculated as total Prox1$^+$ area at corneal limbus. Scale bars: 100 μm (SC); 500 μm (limbal LV). SC and limbal LV area, and expression of each molecule in WT group are normalized to 100%, and their relative levels in *Angpt1*$^{i\Delta/\Delta}$ or *Angpt2*$^{i\Delta/\Delta}$ mice are presented. Each group, n = 3-5. *P < 0.05 versus WT by Mann-Whitney U test.

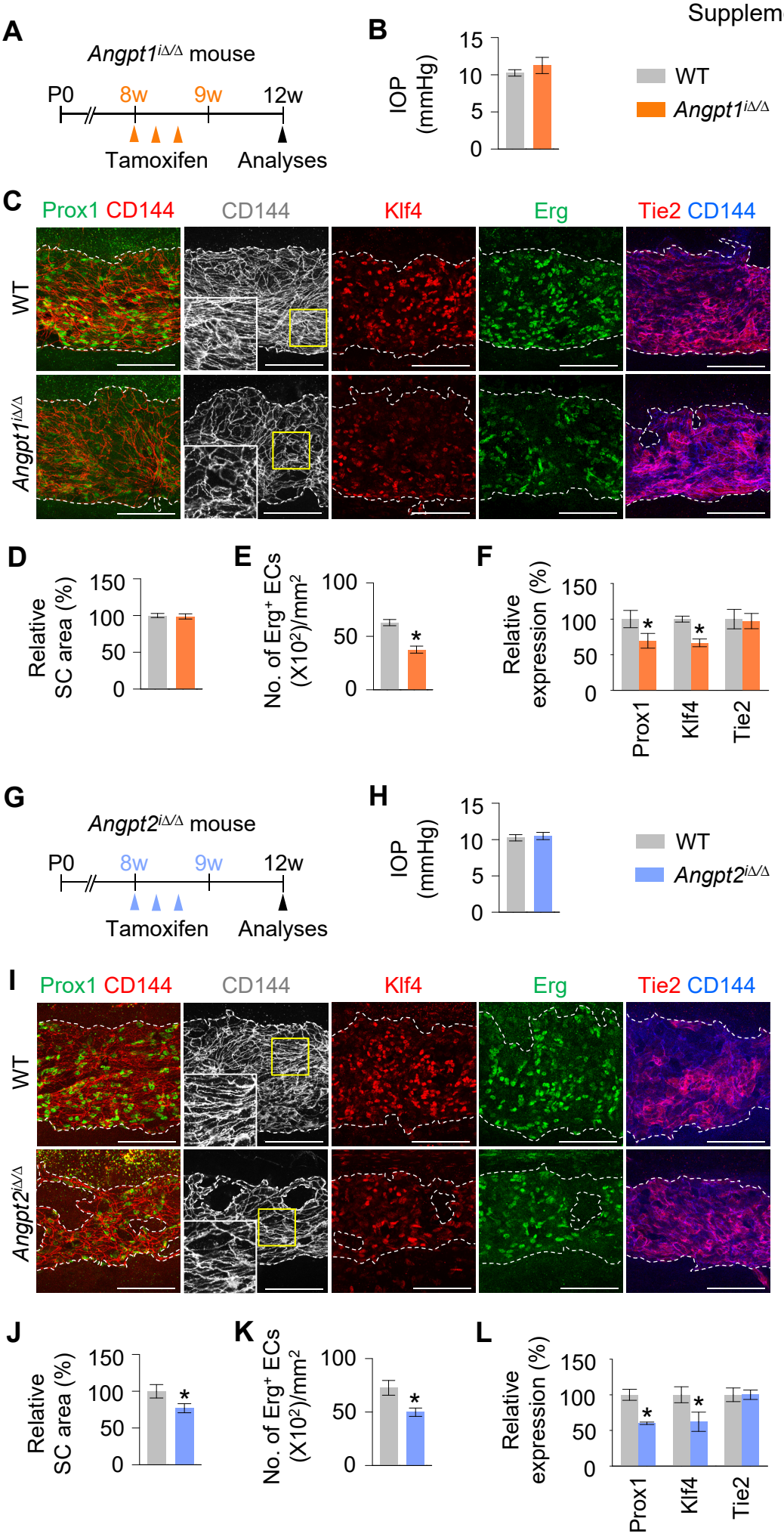
A
Angpt1iΔ/Δ mouse
P0
8w
9w
12w
Tamoxifen
Analyses
B
IOP (mmHg)
15
10
5
0
WT
Angpt1iΔ/Δ
C
Prox1 CD144
CD144
Klf4
Erg
Tie2 CD144
WT
Angpt1iΔ/Δ
D
Relative SC area (%)
150
100
50
0
E
No. of Erg+ ECs (X10²)/mm²
100
50
0
*
F
Relative expression (%)
150
100
50
0
*
*
Prox1
Klf4
Tie2
G
Angpt2iΔ/Δ mouse
P0
8w
9w
12w
Tamoxifen
Analyses
H
IOP (mmHg)
15
10
5
0
WT
Angpt2iΔ/Δ
I
Prox1 CD144
CD144
Klf4
Erg
Tie2 CD144
WT
Angpt2iΔ/Δ
J
Relative SC area (%)
150
100
50
0
*
K
No. of Erg+ ECs (X10²)/mm²
100
50
0
*
L
Relative expression (%)
150
100
50
0
*
*
Prox1
Klf4
Tie2

Supplemental Figure 5. Single depletion of Angpt1 or Angpt2 partially impairs SC integrity during adulthood. (**A** and **G**) Diagram for global depletion of Angpt1 or Angpt2 starting at 8-week old mice and analyses 4 weeks later using *Angpt1*$^{i\Delta/\Delta}$ or *Angpt2*$^{i\Delta/\Delta}$ mice. (**B**-**F** and **H**-**L**) Images and comparisons of IOP, relative area, number of Erg^{+} ECs, and intensities of Prox1, Klf4, and Tie2 immunostaining in CD144^{+} SC. Dashed lines demarcate the margins of SC, and each area marked by a yellow box is magnified in the corner. Scale bars: 100 μm. SC area and expression of each molecule in WT group are normalized to 100%, and their relative levels in *Angpt1*$^{i\Delta/\Delta}$ or *Angpt2*$^{i\Delta/\Delta}$ mice are presented. Each group, $n = 4$. *$P < 0.05$ versus WT by Mann-Whitney *U* test.

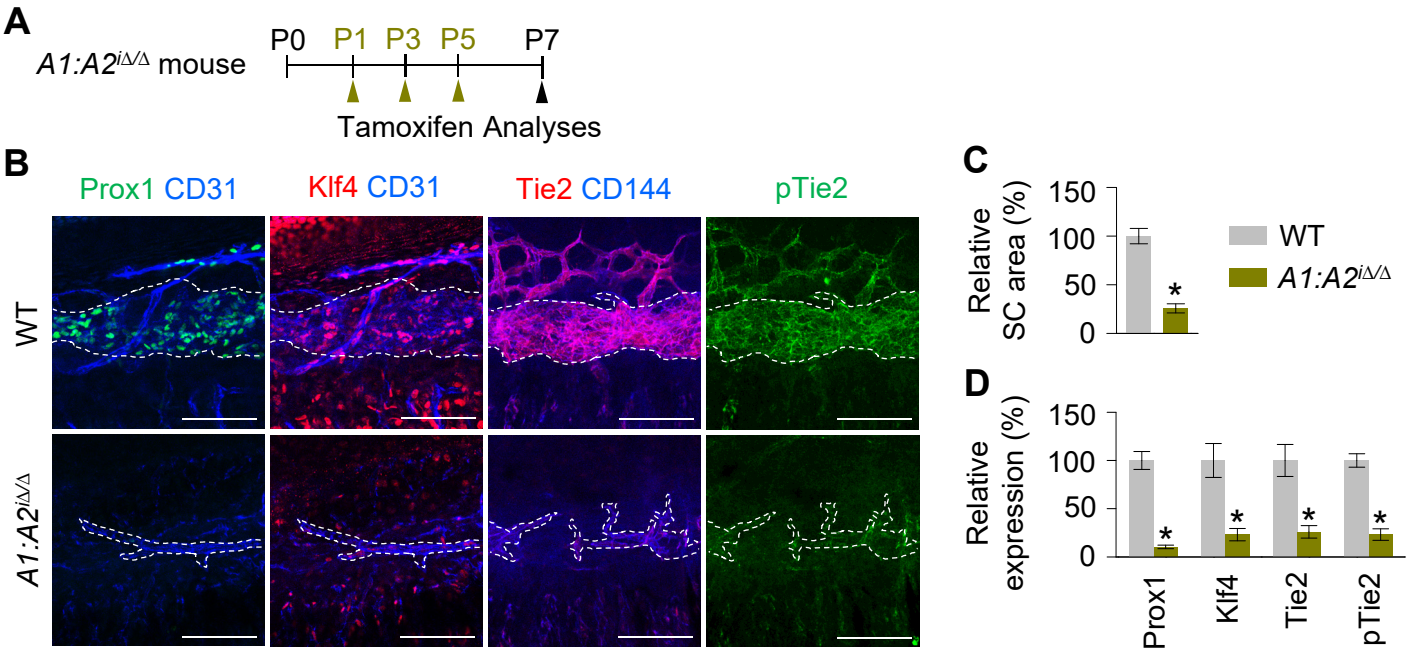

Supplemental Figure 6. Combined depletion of Angpt1 and Angpt2 severely impairs SC formation. (**A**) Diagram for global depletion of Angpt1 and Angpt2 starting at P1 and their analyses at P7 using *A1:A2*$^{i\Delta/\Delta}$ mice. (**B-D**) Images and comparisons of relative area and intensities of Prox1, Klf4, Tie2, and pTie2 immunostaining in CD31$^+$ or CD144$^+$ SC. Dashed lines demarcate the margins of SC. Scale bars: 100 μm. SC area and expression of each molecule in WT mice are normalized to 100%, and their relative levels in *A1:A2*$^{i\Delta/\Delta}$ mice are presented. Each group, n = 4-5. *P < 0.05 versus WT by Mann-Whitney U test.

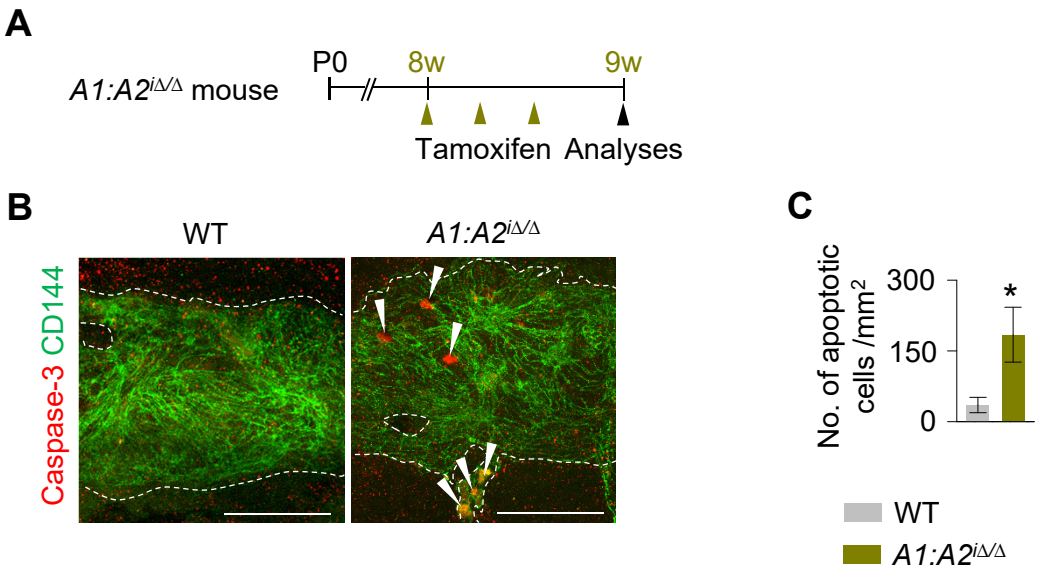

Supplemental Figure 7. Combined depletion of Angpt1 and Angpt2 increases apoptosis of ECs in SC. (**A**) Diagram for global depletion of Angpt1 and Angpt2 starting at 8-week-old mice and analyses 1 week later using *A1:A2*$^{i\Delta/\Delta}$ mice. (**B** and **C**) Images and comparison of number of caspase-3^{+} ECs in SC. Dashed lines demarcate the margins of SC. Scale bars: 100 μm. Each group, n = 5. *P < 0.05 versus WT by Mann-Whitney U test.

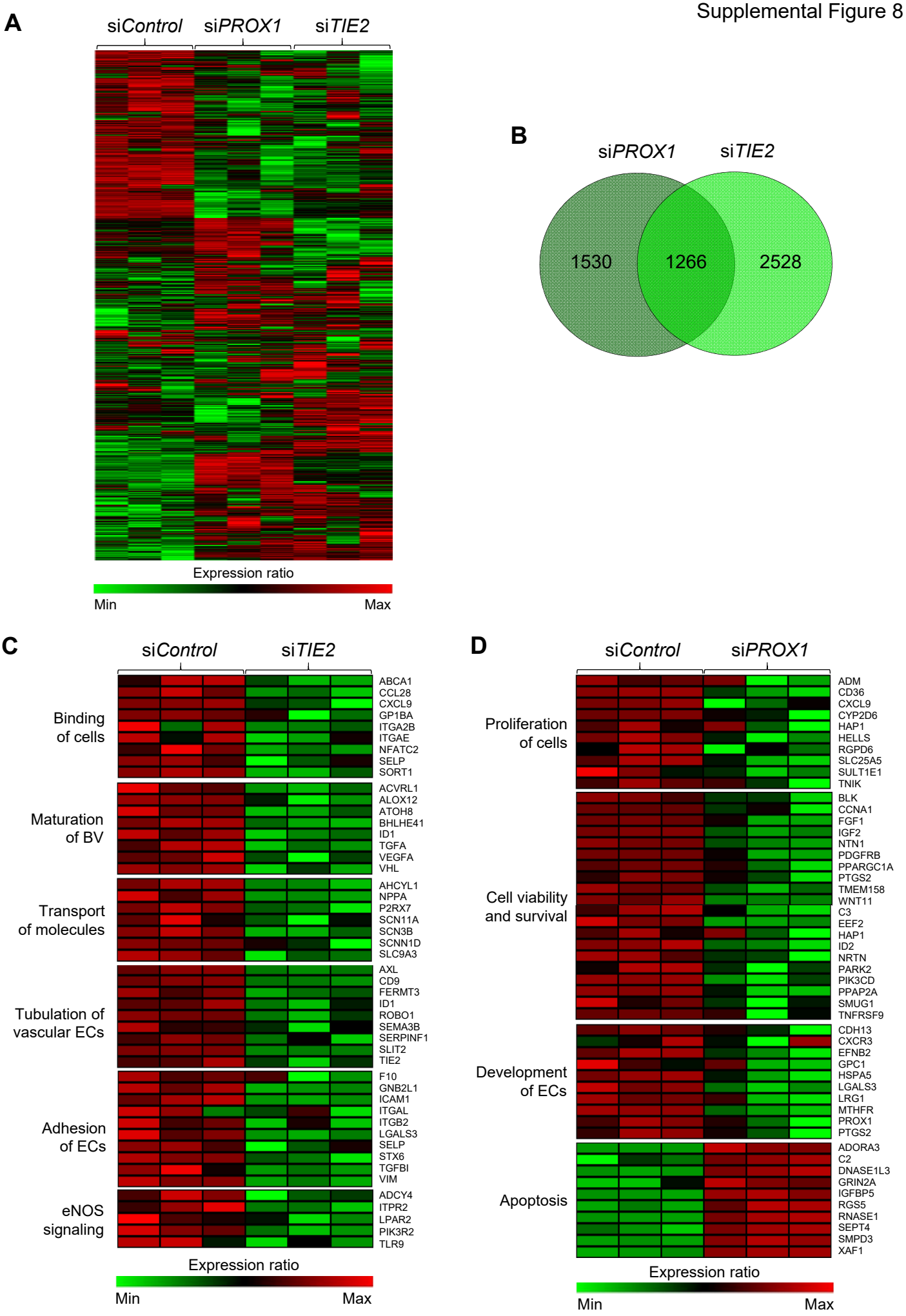
A
siControl
siPROX1
siTIE2
Expression ratio
Min
Max
B
siPROX1
siTIE2
1530
1266
2528
C
siControl
siTIE2
Binding of cells
ABCA1
CCL28
CXCL9
GP1BA
ITGA2B
ITGAE
NFATC2
SELP
SORT1
Maturation of BV
ACVRL1
ALOX12
ATOH8
BHLHE41
ID1
TGFA
VEGFA
VHL
Transport of molecules
AHCYL1
NPPA
P2RX7
SCN11A
SCN3B
SCNN1D
SLC9A3
Tubulation of vascular ECs
AXL
CD9
FERMT3
ID1
ROBO1
SEMA3B
SERPINF1
SLIT2
TIE2
Adhesion of ECs
F10
GNB2L1
ICAM1
ITGAL
ITGB2
LGALS3
SELP
STX6
TGFBI
VIM
eNOS signaling
ADCY4
ITPR2
LPAR2
PIK3R2
TLR9
Expression ratio
Min
Max
D
siControl
siPROX1
Proliferation of cells
ADM
CD36
CXCL9
CYP2D6
HAP1
HELLS
RGPD6
SLC25A5
SULT1E1
TNIK
Cell viability and survival
BLK
CCNA1
FGF1
IGF2
NTN1
PDGFRB
PPARGC1A
PTGS2
TMEM158
WNT11
C3
EEF2
HAP1
ID2
NRTN
PARK2
PIK3CD
PPAP2A
SMUG1
TNFRSF9
Development of ECs
CDH13
CXCR3
EFNB2
GPC1
HSPA5
LGALS3
LRG1
MTHFR
PROX1
PTGS2
Apoptosis
ADORA3
C2
DNASE1L3
GRIN2A
IGFBP5
RGS5
RNASE1
SEPT4
SMPD3
XAF1
Expression ratio
Min
Max

Supplemental Figure 8. RNA sequencing analysis of hDLECs transfected with *TIE2* and *PROX1* siRNAs. RNA sequencing was performed in the hDLECs that were transfected with si*Control*, si*TIE2* or si*PROX1*. DEGs ($P < 0.05$) between each group were analyzed. (**A**) RNA sequencing gene expression heatmap by hierarchical clustering analysis. Those shown in red are upregulated genes and those shown in green are downregulated genes determined by their expression ratio. (**B**) Venn diagram illustrating overlap of DEGs in the si*TIE2* and si*PROX1* genesets. (**C** and **D**) Gene expression heatmap of genes encoding biological functional terms in the si*TIE2* or si*PROX1* geneset.

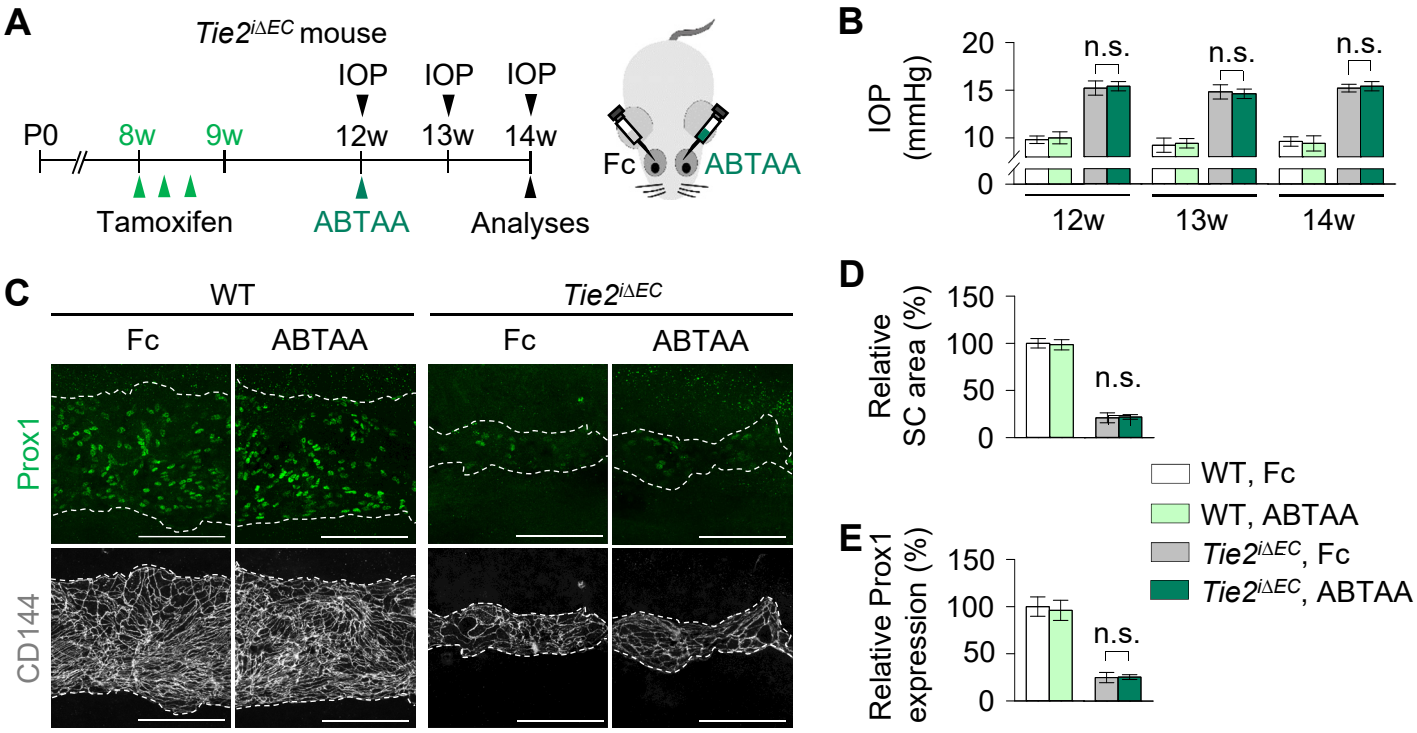

Supplemental Figure 9. Analyses of the effects of ABTAA treatment in adult conditional *Tie2*-depleted SC. (**A**) Diagram depicting the experiment schedule in WT and *Tie2*$^{i\Delta EC}$ mice for administrations of tamoxifen and intraocular ABTAA (~5 µg, left eye) and Fc (~5 µg, right eye), periodic measurements of IOP, and analyses of their SCs. (**B**-**E**) Images and comparisons of IOP, relative area, and intensity of Prox1 immunostaining in CD144^{+} SC. Dashed lines demarcate SC. Scale bars: 100 µm. SC area and expression of each molecule in WT mice treated with Fc are normalized to 100%, and their relative levels of other groups are presented. Each group, *n* = 5. n.s., non-significant by Kruskal-Wallis test followed by Tukey's HSD test with ranks.

Supplemental Table 1. List of siRNA Sequences

Name	Sequence (5’ - 3’)
Human *Control*	UAGCGACUAAACACAUCAA
Human *PROX1*	CCGAGUGCGGCGAUCUUCAAGAUAU
Human *TIE2*	GGCUAGUAAGAUCAAUGGUdTdT

Supplemental Table 2. List of Primer Sets for Quantitative Real-Time RT-PCR

Name	Sequence (5’ - 3’)	
Mouse *GAPDH* (housekeeping gene)	Forward	GTCGTGGAGTCTACTGGTGTCTTCAC
	Reverse	GTTGTCATATTTCTCGTGGTTCACACCC
Mouse *Angpt1*	Forward	CTCTGCAAAGGGATGCTCCACACG
	Reverse	CTGTTGTATCTGGGCCATCTCCGAC
Mouse *Angpt2*	Forward	ACCGGTCAGCACCGCTACGTG
	Reverse	TGCGTCAAACCACCAGCCTCCTG
Human *GAPDH* (housekeeping gene)	Forward	GGTGGTCTCCTCTGACTTCA
	Reverse	GTTGCTGTAGCCAAATTCGT
Human *PROX1*	Forward	CTGAAGACCTACTTCTCCGACG
	Reverse	GATGGCTTGACGTGCGTACTTC
Human *TIE2*	Forward	GTTGACTCTAGCTCGGACCAC
	Reverse	TTGAAGTGGAGAGAAGGTCTG
Human *KLF4*	Forward	GAACTGACCAGGCACTACCG
	Reverse	TTCTGGCAGTGTGGGTCATA
Human *CDH5*	Forward	GGCAAGATCAAGTCAAGCGTG
	Reverse	ACGTCTCCTGTCTCTGCATCG

Supplemental Table 3. Characterization of gene signatures in *Tie2* knockdown hDLECs (excel file name: Supplemental Table 3.xlsx).

Supplemental Table 4. Characterization of gene signatures in *Prox1* knockdown hDLECs (excel file name: Supplemental Table 4.xlsx).